

Minerals Engineering

Mass balance study of a multistage process for the purification of a fluorspar by-product from a rare earth element carbonatite deposit

--Manuscript Draft--

Manuscript Number:	
Article Type:	Research Paper
Keywords:	fluorite, fluorspar, carbonatite, REEs, magnetic separation, acid leaching, flotation, mass balance, economic evaluation
Corresponding Author:	Jean-Francois Blais, Ph.D. INRS Quebec, Quebec CANADA
First Author:	Thi Yen Chau Nguyen, M.Sc.
Order of Authors:	Thi Yen Chau Nguyen, M.Sc. Lan Huong Tran, Ph.D. Lucie Coudert, Ph.D. Kristin K Mueller, Ph.D. Guy Mercier, Ph.D. Jean-Francois Blais, Ph.D.
Abstract:	<p>Fluorspar, also known as fluorite (CaF_2), is commercially important in metallurgical (e.g. used as slag viscosity modifier), ceramic (e.g. used to manufacture glass), and chemical industries (e.g. production of commercial HF). In the present study, a process has been developed to produce a ceramic grade fluorspar by-product from a rare earth element (REE)-bearing carbonatite deposit. The objective of the present study was to conduct a mass balance assessment of a CaF_2 by-product purification process as well as an economic evaluation of the final flotation step to determine the advantage/limitation of this additional step to improve the purity of CaF_2 from metallurgical to ceramic grade. After an initial flotation step to produce feed, the fluorspar purification process consisted of four steps. Firstly, a magnetic separation step was conducted to pre-concentrate the fluorspar into a non-magnetic fraction, while concentrating Fe- and REE-bearing minerals in the magnetic fraction. Secondly, the non-magnetic fraction was subjected to an acid leaching step to solubilize carbonates. Thirdly, the leached solid was treated again by magnetic separation to remove the further liberated REE-bearing minerals from the fluorspar minerals. Finally, a flotation step was performed to depress silicate minerals in the tailings fraction and thus to improve fluorspar grade in the concentrate. The purity of fluorspar increased from 15.6% in the feed (no commercial value, residue to be disposed of) to 95.1% in the final product (ceramic grade). According to the mass balance calculations, approximately 98.6 g of ceramic grade CaF_2 was recovered from 1 kg of feed material and the output/input ratio of fluorspar was estimated at 94.0%. The costs of the flotation process developed to improve the purity of CaF_2 from metallurgical to ceramic grade were estimated at 194 \$CAD.t⁻¹, while the revenue to be generated by the ceramic grade fluorspar obtained were estimated at 244 \$CAD.t⁻¹, indicating that the additional flotation step is economically feasible and beneficial to the company, not only to upgrade fluorspar by-product (from commercial to ceramic grade), but also to generate a profit of at least 50 \$CAD.t⁻¹.</p>

Highlights

- Purification of fluorspar by-product from rare earth element carbonatite deposit
- Combination of magnetic separation, acid leaching and flotation
- Increase in purity of fluorspar from 15.6% to 95.1%
- Purification of fluorspar generated a significant cost benefit for rare earth process

1
2
3
4
5 1
6
7
8 2 **Mass balance study of a multistage process for the purification of a fluorspar by-**
9
10 3 **product from a rare earth element carbonatite deposit**
11
12
13 4
14

15 5 Thi Yen Chau Nguyen^a, Lan Huong Tran^b, Lucie Coudert^c,

16
17 6 Kristin K. Mueller^d, Guy Mercier^e, Jean-François Blais^{f*}
18
19
20 7
21

22
23 8 ^a Ph.D Student, Institut National de la Recherche Scientifique (Centre Eau Terre Environnement),
24 9 Université du Québec, 490 Rue de la Couronne, Québec, QC, Canada G1K 9A9, Phone: (418) 654-2530
25 10 ext. 4472, Fax: (418) 654-2600, email: thi_yen_chau.nguyen@ete.inrs.ca
26

27 11 ^b Research Associate, Institut National de la Recherche Scientifique (Centre Eau Terre Environnement),
28 12 Université du Québec, 490 rue de la Couronne, Québec, QC, Canada, G1K 9A9, Phone: (418) 654-
29 13 2550, Fax: (418) 654-2600, email: lan.huong.tran@ete.inrs.ca
30

31 14 ^c Assistant Professor, Université du Québec en Abitibi-Témiscamingue (Institut de Recherche en Mines
32 15 et Environnement), 445 boulevard de l'Université, Rouyn-Noranda, QC, Canada, J9X 5E4, Phone:
33 16 (819) 762-0971 ext. 2572, Fax: (819) 797-4727, email: lucie.coudert@ugat.ca
34

35 17 ^d Research Associate, Institut National de la Recherche Scientifique (Centre Eau Terre Environnement),
36 18 Université du Québec, 490 rue de la Couronne, Québec, QC, Canada, G1K 9A9, Phone: (418) 654-
37 19 3793, Fax: (418) 654-2600, email: kristin.mueller@ete.inrs.ca
38

39 20 ^e Professor, Institut National de la Recherche Scientifique (Centre Eau Terre Environnement),
40 21 Université du Québec, 490 rue de la Couronne, Québec, QC, Canada, G1K 9A9, Phone: (418) 654-
41 22 2633, Fax: (418) 654-2600, email: guy.mercier@ete.inrs.ca
42

43 23 ^f Professor, Institut National de la Recherche Scientifique (Centre Eau Terre Environnement),
44 24 Université du Québec, 490 rue de la Couronne, Québec, QC, Canada, G1K 9A9, Phone: (418) 654-
45 25 2575, Fax: (418) 654-2600, email: blaisjf@ete.inrs.ca
46
47 26

48
49 27 * Corresponding author
50
51
52 28
53
54
55
56
57
58
59
60
61
62
63
64
65

1
2
3
4 **29 Abstract**

5
6
7
8 30 Fluorspar, also known as fluorite (CaF₂), is commercially important in metallurgical (e.g. used as slag
9 31 viscosity modifier), ceramic (e.g. used to manufacture glass), and chemical industries (e.g. production of
10 32 commercial HF). In the present study, a process has been developed to produce a ceramic grade fluorspar
11 33 by-product from a rare earth element (REE)-bearing carbonatite deposit. The objective of the present
12 34 study was to conduct a mass balance assessment of a CaF₂ by-product purification process as well as an
13 35 economic evaluation of the final flotation step to determine the advantage/limitation of this additional
14 36 step to improve the purity of CaF₂ from metallurgical to ceramic grade. After an initial flotation step to
15 37 produce feed, the fluorspar purification process consisted of four steps. Firstly, a magnetic separation step
16 38 was conducted to pre-concentrate the fluorspar into a non-magnetic fraction, while concentrating Fe- and
17 39 REE-bearing minerals in the magnetic fraction. Secondly, the non-magnetic fraction was subjected to an
18 40 acid leaching step to solubilize carbonates. Thirdly, the leached solid was treated again by magnetic
19 41 separation to remove the further liberated REE-bearing minerals from the fluorspar minerals. Finally, a
20 42 flotation step was performed to depress silicate minerals in the tailings fraction and thus to improve
21 43 fluorspar grade in the concentrate. The purity of fluorspar increased from 15.6% in the feed (no
22 44 commercial value, residue to be disposed of) to 95.1% in the final product (ceramic grade). According to
23 45 the mass balance calculations, approximately 98.6 g of ceramic grade CaF₂ was recovered from 1 kg of
24 46 feed material and the output/input ratio of fluorspar was estimated at 94.0%. The costs of the flotation
25 47 process developed to improve the purity of CaF₂ from metallurgical to ceramic grade were estimated at
26 48 194 \$CAD.t⁻¹, while the revenue to be generated by the ceramic grade fluorspar obtained were estimated
27 49 at 244 \$CAD.t⁻¹, indicating that the additional flotation step is economically feasible and beneficial to the
28 50 company, not only to upgrade fluorspar by-product (from commercial to ceramic grade), but also to
29 51 generate a profit of at least 50 \$CAD.t⁻¹.

30
31
32
33
34
35
36
37
38
39
40
41
42
43
44
45
46
47
48
49
50 53 **Keywords:** fluorite, fluorspar, carbonatite, REEs, magnetic separation, acid leaching, flotation, mass
51 54 balance, economic evaluation

1 Introduction

More than 500 carbonatite occurrences have been found around the world, mainly in the East African Rift zone, eastern Canada, northern Scandinavia, the Kola Peninsula in Russia and southern Brazil (Woolley and Kjarsgaard, 2008). The carbonatites, mainly (> 50%) composed of carbonate minerals (e.g. calcite and dolomite), contain valuable metals (e.g. rare earth elements -REEs, Zr, Nb, Ta) and industrial minerals (e.g. fluorspar – CaF₂), that are useful for the development of modern high-tech products used in our daily life (Council, 2002). Fluorite, also known as fluorspar, is classified as metallurgical, ceramic or acid grade depending on its quality and specification (Eurofluor, 2016). Metallurgical grade fluorspar contains 60–85% CaF₂ (maximum 15% SiO₂) and is mainly used as a flux to lower the melting temperature of steel, to enhance the fluidity of the slag in ferrous metallurgical and to remove impurities (e.g. sulphur and phosphorus) from molten metals. Ceramic grade fluorspar contains 80–96% CaF₂ (maximum 3% SiO₂) and is mainly used in the production of opaque glass and cooking enamels. Acid grade fluorspar contains more than 97% CaF₂ (maximum 1% SiO₂) and is mainly used either in the manufacturing of hydrofluoric acid (HF) or as a feed stock for many different chemical processes (Hayes et al., 2017). Approximately one third of the world’s fluorspar production is of metallurgical grade while only a small proportion is ceramic grade. The price for each grade is variable, but acid grade typically represents the highest price (CAD\$ 400 to CAD\$ 500 t⁻¹) and the highest volume (4.5 Mt per year, corresponding to 2/3 of the world’s fluorspar production) (Harben, 2002; USGS, 2020). The largest producers of fluorspar associated with carbonatite deposits are located at Okorosu (Namibia), Amba Dongar (India) and Mato Preto (Brazil) (Magotra et al., 2017). However, significant amounts of gangue minerals (e.g. carbonates, silicates) totally liberated or associated to fluorspar cause major problems in the beneficiation steps.

Several methods have been used to pre-concentrate minerals of interest, including fluorspar, from carbonatite-type deposits (Bian et al., 2011; Habashi, 2013; Amine et al., 2019). Usually, beneficiation processes include physical methods (e.g. flotation, magnetic separation and/or gravimetric separation) in conjunction with chemical leaching to remove carbonate minerals (Mat Suli et al., 2017). The choice of an appropriate method depends on the mineralogy and degree of liberation of the minerals (valuable and gangue minerals). Minerals with similar physical properties and chemical behavior require multistage processes in the appropriate order to achieve both an efficient recovery and a high economic grade product (Wenliang & Bingyan, 2011; Filippov et al., 2016; Xiong et al., 2018). The optimal combination of different processes varies from one mine site to another one. For example, the beneficiation flowsheet of the Shizhuyuan deposit consists of many stages of conditioning and flotation combined with six or more

1
2
3
4
5
6
7
8
9
10
11
12
13
14
15
16
17
18
19
20
21
22
23
24
25
26
27
28
29
30
31
32
33
34
35
36
37
38
39
40
41
42
43
44
45
46
47
48
49
50
51
52
53
54
55
56
57
58
59
60
61
62
63
64
65

87 stages of cleaner flotation to produce a fluorspar purity of 93% (Han et al., 2017). Liu et al. (2019) propose
88 a novel approach based on the use of HCl leaching and reverse flotation of sulfide to improve the grade
89 of fluorspar from 93.2 to 97.0%, with a slight loss of fluorspar.

90 The Ashram Rare Earth Deposit is located in northern Quebec, Canada. To pre-concentrate a fluorspar by-
91 product produced from the extraction of the rare earth element carbonatite deposit, a combination of
92 magnetic separation and acid leaching resulted in the upgrading of a low grade fluorspar (16.5%) to a
93 metallurgical grade fluorspar (76.5%). The optimum conditions for each step are detailed in Nguyen et al.
94 (2020). For the magnetic separation, the optimum conditions were three consecutive passes at
95 5,000 Gauss. For the HCl leaching, optimal conditions were as follow: temperature of 20°C, HCl
96 concentration of 5 M and reaction time of 1 hour. Nguyen et al. (2021) also demonstrated that the purity
97 of fluorspar increased from metallurgical grade (76.5%) to ceramic grade (88.6%) with the addition of
98 column flotation. The optimum conditions were as follow: 3.6 g/kg of sodium oleate as the collector,
99 2 g/kg of sodium silicate as the depressant, 35 min of conditioning time, 7 min of flotation time, and a
100 slurry density of 5%. Based on previous results (Nguyen et al., 2020; Nguyen et al. 2021), the present study
101 focuses on the mass balance of the entire fluorspar process, consisting of magnetic separation, acid
102 leaching and direct flotation, to selectively recover a high-grade fluorspar by-product from a REE
103 carbonatite deposit.

2 Materials and methods

2.1 Purification of the fluorspar by-product from a REE carbonatite deposit

106 The raw materials originate from a REE carbonatite deposit (Ashram Deposit – Commerce Resource Corp.)
107 located in northern Quebec, Canada. The Ashram carbonatite deposit consists of different types of
108 mineralization, including REE and fluorspar mineralization at the Ashram Zone. The beneficiation process,
109 mainly designed for the extraction of REEs from this deposit, includes crushing and grinding steps to
110 reduce the particle size to 30 µm and to release useful particle (REE-bearing minerals, fluorspar) from the
111 gangues, followed by a flotation step to separate REE-bearing and fluorspar minerals from the gangue.
112 Sixty kilograms of flotation concentrate from a feasibility pilot scale study was used as the feed (called
113 “initial sample”) in the present paper. The initial sample was mixed for 15 min in a 200 L-capacity drum
114 tumbler combined with corner over corner mixing to obtain a homogeneous sample.

1
2
3
4
5
6
7
8
9
10
11
12
13
14
15
16
17
18
19
20
21
22
23
24
25
26
27
28
29
30
31
32
33
34
35
36
37
38
39
40
41
42
43
44
45
46
47
48
49
50
51
52
53
54
55
56
57
58
59
60
61
62
63
64
65

115 Afterward, the initial sample (S0) was subjected to a 4-step purification process designed to improve the
116 final grade of the fluor spar by-product (Figure 1). Firstly, a magnetic separation step was applied to pre-
117 concentrate the fluor spar into the non-magnetic fraction, while the Fe- and REE-bearing minerals
118 remained in the magnetic fraction. Secondly, the non-magnetic fraction was subjected to an acid leaching
119 step to solubilize the carbonates. Thirdly, the leached solid was subjected to a second magnetic separation
120 step to remove REE-bearing minerals from the pre-concentrated fluor spar. Finally, flotation was
121 employed to depress silicate minerals in tailings fraction and thus to upgrade the fluor spar content in the
122 final concentrate. The optimum conditions for each of the steps of the fluor spar purification process
123 (magnetic separation, acid leaching and column flotation) were defined in previous studies (Nguyen et al.,
124 2020, 2021). The complete fluor spar purification process was carried out in triplicate to confirm the results
125 obtained from the individual steps and to calculate the mass balance of the entire purification process
126 using 1 kg of feed material.

127 **Step 1 - Wet High Intensity Magnetic Separation**

128 The magnetic fraction containing ferromagnetic and paramagnetic particles was separated from the non-
129 magnetic particles using a wet high intensity magnetic separator (WHIMS - CARPCO 3 x 4 L, Outokumpu
130 Technology, Jacksonville, FL, USA). A pump was used to feed the slurry with a solid/liquid (S/L) ratio of
131 25% (w.v⁻¹) through the WHIMS at a flow rate of 0.35 L.min⁻¹. The non-magnetic particles passed through
132 the iron ball matrix and were collected in a box underneath the separation chamber. This operation was
133 repeated three times to attain three subsequent passes at an intensity of 5,000 Gauss. Magnetic particles,
134 attracted to the iron ball matrix, were collected in a different box by reducing the magnetic intensity to
135 zero and were cleaned with water. Following their collection, the magnetic (S1) and non-magnetic (S2)
136 fractions were left to settle for 2 h, filtered, dried at 60°C, and weighed. Samples of the S1 and S2 fractions
137 were collected for further analysis to determine the content of elements of interest in each fraction and
138 estimate their recovery. The input and output of this step are presented in Figure 2a.

139 **Step 2 – Acid leaching**

140 The non-magnetic fraction (S2) was used as feed material for the subsequent acid leaching step. The
141 leaching experiments were conducted in a 4 L beaker (made of acrylic material) using a mechanical stirrer
142 for agitation. Operating conditions were set as following: 5 M HCl, a S/L ratio of 25% (w.v⁻¹), 1 h of a
143 reaction time, ambient temperature and 400 rpm as mixing speed. Following the leaching step, the solids
144 were decanted for 1 h and separated from the leachate (L1). The solid phase was rinsed three times with
145 deionized water (ratio of 25% w.v⁻¹), filtered, dried in an oven at 60°C for 24 h, weighed, digested, and

1
2
3
4 146 analyzed to determine their chemical composition. The input and output of this step are presented in
5
6 147 [Figure 2b](#).

8 148 **Step 3 - Wet High Intensity Magnetic Separation**

10 149 The leached solid (S3) was used as feed material for the subsequent wet high intensity magnetic
11
12 150 separation step. This step separated the magnetic fraction containing paramagnetic REE-bearing particles
13
14 151 from the non-magnetic fraction containing fluor spar in one pass at 3,000 Gauss. A pump was used to feed
15
16 152 the slurry with a S/L ratio of 25% (w.v⁻¹) through the magnetic separator at a flow rate of 0.35 L.min⁻¹.
17
18 153 Magnetic particles, attracted to the sphere media matrix, were collected by reducing the magnetic
19
20 154 intensity to zero and were cleaned with water. After collection, the magnetic (S4) and non-magnetic (S5)
21
22 155 fractions were decanted for 1 h, filtered, dried at 60°C for 24 h, and weighed. The final contents of
23
24 156 elements of interest in S4 and S5 were determined and the recovery of CaF₂ in S5 was estimated. The
25
26 157 input and output of this step are presented in [Figure 2c](#).

27 158 **Step 4 - Column flotation**

29 159 The depression of silicate minerals in the non-magnetic (S5) fraction was carried out using the column
30
31 160 flotation ([Nguyen et al., 2021](#)). Firstly, a slurry was prepared by adding the pre-concentrated fluor spar
32
33 161 (S5) to water with density of 5% (w.v⁻¹). The depressant, sodium silicate (2 g.kg⁻¹), and the collector,
34
35 162 sodium oleate (3.6 g.kg⁻¹), were added to the slurry. The pH was measured after a 30 min conditioning
36
37 163 period. The slurry was then transferred to the column and was left to float for 7 min. The non-float (tailing)
38
39 164 (S6) and the float (fluor spar concentrate) (S7) fractions were the left to decant for 1 h. The tailings fraction
40
41 165 (S6) and the fluor spar concentrate (S7) fraction were rinsed in deionized water with a solid-liquid ratio of
42
43 166 25% (w.v⁻¹), dried at 60°C for 24 h and digested to determine their chemical composition. The input and
44
45 167 output of this step are presented in [Figure 2d](#).

46 168 **2.2 Analytical techniques**

48 169 Mineralogical characterizations were performed by an external laboratory (Activation Laboratories,
49
50 170 Ontario, Canada). Because of the expensive costs related to this analysis, the mineralogical
51
52 171 characterization was used only for the initial sample (S0) to better predict its behavior during physical and
53
54 172 chemical treatment. XRD analyzes were also performed by an external laboratory (XRD-Siemens, Model
55
56 173 D5000, Department of Mining, Metallurgy and Materials Engineering, University of Laval) for the samples
57
58 174 obtain after each step of the process to identify and quantify the mineral phases present. Scans were
59
60 175 acquired for 30 min with position of 2θ ranging from 5° to 85°, scanning step size of 2θ equal 0.02° with a

1
2
3
4
5
6
7
8
9
10
11
12
13
14
15
16
17
18
19
20
21
22
23
24
25
26
27
28
29
30
31
32
33
34
35
36
37
38
39
40
41
42
43
44
45
46
47
48
49
50
51
52
53
54
55
56
57
58
59
60
61
62
63
64
65

176 scan time of 48s per step, with anode material of Cu (40 kV, 8 mA). Matches were obtained using Bruker
177 identification software X'Pert HighScore.

178 Total carbon content was determined using a CHNS Elemental Analyser (LECO TruSpec[®], Model Micro
179 CHNS A). Fusion in the presence of lithium metaborate was used to digest 0.1 g of sample to solubilize the
180 fluoride ions and the other elements from the solid matrix. The fuseate was then dissolved in dilute acids
181 (HNO₃/HCl) and the ionic strength was adjusted with a buffer. The fluorine content of the samples were
182 measured using a multimeter (Accumet Fisher Scientific, Model XL600) equipped with a fluoride electrode
183 (Thermo Scientific, Orion). The chemical composition of the samples was determined in our laboratories
184 using an Inductively Coupled Plasma-Atomic Emission Spectroscopy (ICP-AES, Varian, Model Vista-AX
185 CCO).

186 2.3 Calculations

187 The percentage of recovery (R) of an element was calculated at each step of the process by comparing
188 the mass of an element in the final sample with the one measured in the feed (Equation 1):

189
190 **Equation 1**
$$R (\%) = \frac{\text{Final element concentration } \left(\frac{\text{mg}}{\text{kg}}\right) \times \text{sample mass proportion } (\%)}{\text{Initial element concentration in the feed } \left(\frac{\text{mg}}{\text{kg}}\right)}$$

191
192 The mineralogical composition of the feed sample (S0) showed that almost all the fluoride present in the
193 sample can be associated to the presence of fluorspar (CaF₂) and only a small amount is present in
194 bastnasite (<1.9% of total F), apatite (<0.3% of total F) and biotite (<0.1% of total F). Because these
195 quantities can change throughout the purification process by less than 2%, the fluorspar content was
196 estimated from the fluorine content using Equation 2 (Kampf, 2003):

197
198 **Equation 2**
$$[CaF_2] = [F] \times 2.055$$

201 3 Results and discussion

202 3.1 Characterization of the initial sample (S0)

203 The mineralogical characterization of the initial sample (S0) is shown in Figure 3. The sample contained a
204 large amount of fluor spar (15.6%), while the two main REE-bearing minerals identified, monazite (4.02%)
205 and bastnaesite (1.68%), were present in smaller amounts. The major gangue mineral phases were
206 carbonate (37.9% dolomite Fe, 17.4% ankerite, 7.53% siderite-magnesite, and 2.86% siderite), and
207 silicates (2.23% of quartz). These results are in accordance with the chemical analysis of the representative
208 initial sample (S0) (Table 1). Indeed, the major elements were Ca (21.8%), Mg (5.94%), Fe (6.98%), Si
209 (1.44%), C (7.13%), and F (9.14%).

210 3.2 Mass balance of the overall fluor spar purification process

211 The mass balance of different input and output of the fluor spar purification process developed is shown
212 in Figure 2. The chemical composition of the feed (S0) and each of the solid samples (S1 to S7) produced
213 by the different purification steps is presented in Table 1.

214 Step 1 - Wet High Intensity Magnetic Separation

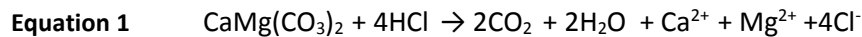
215 The first purification step consisted of 3-consecutive wet high intensity magnetic separation steps,
216 allowing the recovery of two different fractions: i) the magnetic fraction (S1) that represented 50.5% of
217 the weight of the initial sample, and ii) the non-magnetic fraction (S2) that represented 40.4% % of the
218 weight of the initial sample (Figure 2a). A small mass loss (9.1%) was observed during this step, which can
219 be attributed to either the washing step or the solid/liquid separation step (loss of solid particles on the
220 filter). Compared to the initial sample (S0), fluor spar and silicate minerals were enriched in the non-
221 magnetic fraction (S2). Indeed, the fluorine content increased from 9.14% in S0 to 17.5% in S2,
222 corresponding to an increase of CaF₂ content from 18.8% in S0 to 35.9% in S2. The Si content increased to
223 2.46% in S2 and decreased to 0.54% in the magnetic fraction (S1). This can be explained by the non-
224 magnetic properties of fluor spar and quartz when subjected to a magnetic field; the magnetic
225 susceptibility of fluor spar and quartz was $-0.01 \cdot 10^{-3}$ and $-0.6 \cdot 10^{-8} \text{ m}^3 \text{ kg}^{-1}$, respectively (Rosenblum &
226 Brownfield, 2000). However, 4.71% of the F, corresponding to 9.7% of CaF₂ remained in the magnetic
227 fraction (S1). This can be explained by the association of the fluor spar with the other magnetic minerals.
228 According to the mineral liberation analysis, 62.7% of fluor spar was present in a liberated form, while the
229 remaining fluor spar was associated with monazite (3.42%), dolomite (13.9%), ankerite (9.09%), siderite

1
2
3
4
5
6
7
8
9
10
11
12
13
14
15
16
17
18
19
20
21
22
23
24
25
26
27
28
29
30
31
32
33
34
35
36
37
38
39
40
41
42
43
44
45
46
47
48
49
50
51
52
53
54
55
56
57
58
59
60
61
62
63
64
65

230 (2.01%), calcite (3.90%), and other minerals (4.98%). The Fe content increased from 6.98% in S0 to 8.28%
231 in S1, while decreasing to 4.84% in S2. The REE content was 2.77% in S1 and 2.21% in S2, explained by the
232 paramagnetic properties of REE-bearing minerals when subjected to a magnetic field (Jordens et al.,
233 2014). However, as only 55.8% of REE-bearing minerals were fully liberated in S0, 36.5% of REEs from S0
234 were recovered in S2. This can be explained by the association between REEs and the other minerals.
235 According to the mineral liberation data for S0, dolomite (11.9%), ankerite (8.16%), and fluorite (6.18%)
236 were the minerals mainly associated with monazite, while dolomite (10.2%), fluorite (7.37%), ankerite
237 (5.14%), and monazite (1.29%) were mainly associated with monazite. The main purpose of the first
238 magnetic separation step in the process was to remove Fe-bearing carbonates (e.g. siderite, ankerite,
239 dolomite-Fe) from the fluorite by-product before HCl leaching to reduce acid consumption and
240 operating costs. An additional magnetic separation step after the HCl leaching can improve the recovery
241 of less liberated REE-bearing minerals associated with carbonate gangue minerals.

242 Step 2 - Acid leaching to solubilize carbonate minerals

243 The non-magnetic fraction (S2) was used as feed material for the acid leaching step. Sixty percent of the
244 mass was lost, most likely due to the solubilization of carbonate minerals under acidic conditions (Chou
245 et al., 1989; Solihin et al., 2018) (Equation 3).



248
249 This dissolution was accompanied by the release of large amounts of CO_2 (g) and some metals (e.g. Ca, Fe,
250 Mg) associated with carbonate minerals. Indeed, according to the chemical composition results (Table 1),
251 the carbon content decreased from 7.14 (S2) to 0.19% (S3) after the acid leaching step. The contents of
252 Mg and Fe decreased from 4.84 to 0.35% and from 4.26 to 0.40%, respectively. In contrary, F and Si
253 contents increased from 17.5 to 37.0% and from 2.46 to 5.07% in S2 (feed) and S3 (leached residue),
254 respectively. This increase in F and Si content was mainly due to the important reduction of the total mass
255 of the residues (from 404 g to 162 g) during this leaching step and the low solubility of fluorite and
256 silicate minerals under hydrochloric conditions (Crundwell, 2017; Momota et al., 2004; Patnaik, 2002). In
257 addition to the increase in fluorite purity (from 35.9 to 76%), the contents of REEs increased from 2.21
258 to 3.91% in S2 and S3, respectively. This increase can be explained by the fact that REE-bearing minerals
259 are insoluble in acidic conditions and require more aggressive conditions (e.g. acid baking at high

1
2
3
4
5
6
7
8
9
10
11
12
13
14
15
16
17
18
19
20
21
22
23
24
25
26
27
28
29
30
31
32
33
34
35
36
37
38
39
40
41
42
43
44
45
46
47
48
49
50
51
52
53
54
55
56
57
58
59
60
61
62
63
64
65

260 temperature) to transform insoluble bastnasite and monazite into soluble REE-bearing sulfates and/or
261 oxides (Amine et al., 2019; Kursun et al., 2016; Mat Suli et al., 2017). The presence of REEs and Si in higher
262 concentrations in S3 (compared to S2) is not desirable, as these elements represent non-negligible
263 impurities in the fluor spar by-product. Therefore, additional treatment processes are required to remove
264 REE- and Si-bearing minerals from the fluor spar by-product. Because of the similar flotation conditions of
265 REE-bearing minerals (e.g. bastnasite, monazite) and fluor spar (Minz et al., 2017; Wenliang & Bingyan,
266 2011), the leached solid (S3) was submitted once again to magnetic separation to remove these minerals,
267 and increase their recovery before the flotation step used to remove residual silicates.

268 **Step 3 - Wet High Intensity Magnetic Separation**

269 The leached solid (S3) was transferred to the WHIMS to remove residual paramagnetic REE-bearing
270 minerals. After the second magnetic separation, the mass recovery was estimated at 93.4%, with 5.8%
271 (9.35 g) recovered in the magnetic fraction (S4) and 87.7% (142 g) recovered in the non-magnetic fraction
272 (S5) (Figure 2c). The 6.6% mass loss may be due to the washing step (difficulty to separate the magnetic
273 particles from the iron balls) or the solid/liquid separation step. The fluorine content increased to 39.3%
274 in the non-magnetic fraction (S5), corresponding to 81% of CaF₂ purity. The content of REEs increased to
275 25.9% in the magnetic fraction (S4), while its content decreased to 2.44% in the non-magnetic fraction
276 (S5). X-ray diffraction (XRD) patterns for S4 (magnetic fraction) and S5 (non-magnetic fraction) are
277 presented in Supplementary Figure 1. In the magnetic fraction (S4), the main minerals were fluor spar
278 (60%) and monazite (40%), while the non-magnetic fraction was mainly composed of fluor spar (86%),
279 quartz (11%) and monazite (3%).

280 Based on these results, it can be noted that 38.2% of the residual REEs in S3 were recovered during this
281 second magnetic separation step in the magnetic fraction (S4) with a REE content of 25.9%, while 57.1%
282 of total REEs were recovered in the magnetic fraction (S1) with a lower REE content of 2.77%. This
283 improvement in REE content in the magnetic fraction (S4 vs. S1) can be explained by the fact that HCl
284 reacted with the outer layer of the carbonate particles during the leaching step in which monazite was
285 included, increasing the degree of liberation of paramagnetic REE-bearing minerals. The purpose of this
286 second magnetic separation step (third step of the fluor spar process) was to remove the further liberated
287 REE-bearing minerals from fluor spar by-product, so as to improve the purity of the fluor spar entering in
288 the flotation step and to enhance the recovery of REEs of the overall process from 57.1% to 67.1% in
289 magnetic fractions (S1 and S4).

1
2
3
4
5
6
7
8
9
10
11
12
13
14
15
16
17
18
19
20
21
22
23
24
25
26
27
28
29
30
31
32
33
34
35
36
37
38
39
40
41
42
43
44
45
46
47
48
49
50
51
52
53
54
55
56
57
58
59
60
61
62
63
64
65

291 Step 4 - Column flotation

292 The non-magnetic fraction (S5) from step 3 was used as feed material for the flotation step. The tailing
293 fraction (S6) represented 27.9% of the total mass of the feed material, while the concentrate fraction (S7)
294 represents more than 69.4% of the feed material (Figure 2d). The chemical composition of S7 showed that
295 fluorine and calcium content increased from 38.7 to 45.1% and from 39.3 to 45.7%, respectively, while Si
296 content decreased from 5.55 to 1.15%. On the contrary, Si content increased to 14.9% in the tailings (S6),
297 while the concentrations of Ca and F decreased to 26.9% and 33.4%, respectively. These results indicated
298 that fluor spar minerals were efficiently floated (81.6% of CaF₂ recovery), while silicate minerals were
299 depressed using sodium oleate as collector and sodium silicate as depressant. The flotation efficiency can
300 be explained by the fact that the fluor spar mineral surface was rendered hydrophobic by the
301 chemisorption between the exposed Ca²⁺ on fluor spar surface and carboxyl (-COO-) groups of sodium
302 oleate collector. Moreover, the use of sodium silicate strongly depressed the quartz, improving the
303 separation of CaF₂ from the quartz minerals. The ability of sodium silicate to depress silicate minerals and
304 sodium oleate to float fluor spar has been demonstrated by Ye and Yang (1992) and Corpas-Martínez et
305 al. (2020). More details on flotation performances are presented in a previous study (Nguyen et al., 2021).
306 XRD patterns showed that the concentrate (S7) was mainly composed of fluor spar (95.1%), while trace
307 amounts of La-monazite (1.8%) and quartz (3.1%) were still present (Supplementary Figure 2). The
308 presence of the monazite and quartz in S7 can be explained by the association between fluor spar and
309 REE-bearing minerals and quartz. According to the mineral liberation analysis for S0, 3.42% of fluor spar
310 was associated with monazite and 0.24% of fluor spar was associated with quartz.

311 Overall fluor spar process

312 Based on the results presented above, a ceramic grade CaF₂ by-product (95.1% CaF₂ purity) was obtained
313 from a low-grade and non-commercially viable CaF₂ (15.6% CaF₂ purity) by-product using successive
314 magnetic separation, acid leaching and flotation steps (Figure 1). The mineral character of the samples
315 after each step of the fluor spar process, as interpreted from XRD analyses, is presented in Figure 4.

316 Firstly, the efficiency of magnetic separation to separate fluor spar (non-magnetic minerals) from magnetic
317 minerals was demonstrated by XRD analysis. Indeed, the presence of fluor spar was confirmed in non-
318 magnetic fractions (S2 and S5) by the presence of peaks at 28° and 46.9° as well as 55.6°2θ in high
319 intensities. The absence or the presence of low intensity peaks that are characteristics of fluor spar and
320 quartz in the magnetic fraction (S1 and S4) indicated that magnetic separation was successful, limiting
321 fluor spar and quartz losses in the magnetic fraction. In addition, the efficiency of magnetic separation to

1
2
3
4
5
6
7
8
9
10
11
12
13
14
15
16
17
18
19
20
21
22
23
24
25
26
27
28
29
30
31
32
33
34
35
36
37
38
39
40
41
42
43
44
45
46
47
48
49
50
51
52
53
54
55
56
57
58
59
60
61
62
63
64
65

concentrate paramagnetic REE-bearing minerals was shown by the presence of peaks with high intensities at 18°, 21°, 40° and 41°2θ in S4, which are characteristics of monazite. Secondly, the efficiency of the HCl leaching was demonstrated by the absence of a peak at 30°2θ, which is characteristic of the presence of dolomite in the leached solid (S3) after step 2. Finally, the efficiency of the flotation was demonstrated by the presence of fluor spar high intensity peaks at 28°, 46.9° and 55.6°2θ, the absence of a quartz peak at 26.5°2θ in the concentrate fraction (S7), and by the presence of high intensity quartz peak at 26.5°2θ in the tailings fraction (S6), demonstrating that quartz was efficiently depressed by sodium silicate, while fluor spar was efficiently activated by the use of sodium oleate and floated.

Figure 5 shows the mass balance of inputs and outputs for the complete fluor spar purification process based on the treatment of 1 kg of initial sample. The inputs included the initial sample (S0), the chemical reagents used for leaching (HCl 100%) and flotation (sodium silicate, sodium oleate) and water. The outputs included the magnetic fractions (S1 and S4), the tailings fraction (S6), the ceramic grade fluor spar by-product (S7), gas (e.g. CO₂), as well as leachates from the leaching step and, finally, water. In the current operating state, all process water and acidic solutions collected from the different treatment steps were not recirculated, but this option can be further evaluated in another project to reduce the amounts of liquid waste to be treated and disposed of. In previous studies, the use of recycled rinsing water, counter-current acid leaching, regeneration of HCl and mineral carbonation was employed to reduce the environmental impacts of similar processes, while sometimes creating a secondary source of revenue (Coudert et al., 2013a; Mocellin et al., 2017; Pasquier et al., 2016). From the results presented in Figure 5, it is shown that 98.6 g of fluor spar by-product can be recovered from 1 kg of the initial solid sample entering the process, while consuming 250 g of HCl, 0.51 g of sodium oleate and 0.28 g of sodium silicate. This reveals that the highest quantity of chemical product was used in the leaching step, while the lowest chemical quantity was used in the magnetic separation and the flotation steps. The high consumption of acid in the leaching step is inevitable and allowed the transformation of insoluble REE-bearing minerals into soluble minerals, increasing the potential to recover revenues from the leached residues. In the primary process currently presented for the Ashram project used by CRC, acid leaching was performed before magnetic separation and the quantity of acid used was estimated at 580 g.kg⁻¹ (personal discussion with D. Smith). Therefore, the alternative approach (magnetic separation followed by acid leaching) presented in this paper should be considered to reduce by half the acid consumption as well as reduce the temperature (80 vs. 20°C) needed for the leaching step, and therefore associated operating costs.

1
2
3
4
5
6
7
8
9
10
11
12
13
14
15
16
17
18
19
20
21
22
23
24
25
26
27
28
29
30
31
32
33
34
35
36
37
38
39
40
41
42
43
44
45
46
47
48
49
50
51
52
53
54
55
56
57
58
59
60
61
62
63
64
65

352 Table 2 illustrates the mass balance and overall recovery and grade of the fluorspar by-product and REEs.
353 The chemical composition of the different solid samples collected after each step was used to calculate
354 CaF₂ and REE recovery. If there is no accumulation, loss or contamination during the process the
355 output/input ratio is equal to 100%. In the present study, output/input ratio of the sample mass was not
356 determined because the loss of mass due to the carbonate dissolution and the production of gas CO₂ in
357 step 2 was not quantified. The output/input ratios of fluorspar and REEs were estimated at 94% and 82%,
358 respectively. The loss of particles during the process operation (especially during magnetic separation
359 with the difficulty in removing (para-) magnetic particles from iron balls) or to solid to liquid separation
360 can explain the less than 100% ratio. The REE mass recovery was 67.1% in S1 and S4, 4.8% in S6, 7.0% in
361 S7, and 3.1% in L1. The fluorspar mass recovery was 50.3% in S7, 13.6% in S6 , 27.9% in S1 and S4, and
362 only 0.8% in L1, demonstrating that the addition of the flotation step decreased the recovery of fluorspar
363 from 72.1% to 50.3%, but the purity of fluorspar increased from metallurgical grade (75%) to ceramic
364 grade fluorspar (98.6%). Therefore, an economic evaluation for the flotation step was required to
365 determine if the addition of this step in the fluorspar by-product purification process is beneficial or not
366 in terms of revenue generation.

3.3 Economic evaluation of the fluorspar by-product flotation purification process

368 The fluorspar by-product purification process developed in this study consists of two main treatment
369 processes based on the fluorspar grade obtained and its potential of valorization:

- 370 i) magnetic separation (S1 and S3) and acid leaching (S2) to separate REE-bearing minerals from
371 fluorspar and simultaneously upgrade the fluorspar by-product to the metallurgical commercial
372 category;
- 373 ii) column flotation (S4) to remove residual silicate minerals from the fluorspar by-product and
374 increase its final quality (ceramic grade).

375 An economic evaluation was not considered for the first treatment process in this paper because the
376 potential of REEs has yet been valorized to the commercial grade in this process. However, a preliminary
377 economic assessment for the primary process currently presented for Ashram project for the recovery of
378 REEs (acid leaching followed by magnetic separation), has been performed despite the lack of valorization
379 of fluorspar as a potential by-product (Gagnon, 2015). Therefore, the economic evaluation in the present
380 paper focused on the second part of the process to demonstrate the potential of an additional flotation

1
2
3
4
5
6
7
8
9
10
11
12
13
14
15
16
17
18
19
20
21
22
23
24
25
26
27
28
29
30
31
32
33
34
35
36
37
38
39
40
41
42
43
44
45
46
47
48
49
50
51
52
53
54
55
56
57
58
59
60
61
62
63
64
65

381 step, not only to upgrade the fluorspar by-product grade from a metallurgical grade to a ceramic grade,
382 but also to create a secondary source of revenue for the company.

383 For this study, a simulation was completed to estimate the economic performance of this flotation process
384 in terms of direct and indirect costs. The simulation included approximately 260 input variables to define
385 the various processing steps, capitalization, and operating parameters. The economic scenario evaluated
386 the direct and indirect costs for the flotation process with a treatment capacity of 100 t.d⁻¹, with a running
387 time of 24 h.d⁻¹, an annual operating period of 350 d.yr⁻¹ and an operating efficiency factor of 95%
388 (Table 3).

389 Total costs were determined based on variable equations including the dimension and treatment capacity
390 of required equipment, purchase costs and the transport of these equipment, electric and thermal
391 requirements, as well as energy consumption, as recorded in previous studies (Metahni et al., 2020; Tran
392 et al., 2020). Depreciation and annual interest charges were estimated using a 20-year equipment lifetime,
393 as well as a working capital of 15% of fixed capital costs. In addition, used market parameters were defined
394 as follows: an inflation rate of 2%, an annual interest rate of 5%, and an annual discount rate of 6%.

395 A 20% Safety Factor was used while sizing the equipment to consider the operational fluctuations that
396 can be encountered on the industrial scale (Remer and Chai, 1990). The cost to purchase (including
397 transport) the various equipment (CATE) constituting the treatment chain was estimated using
398 Equation 4.

399
400 **Equation 2**
$$CATE = X * [(CAP)]^Y * (CEPCI)_{(a/o)}$$

401
402 Where « X » is the constant determined from a power law regression of equipment prices for different
403 capacities (CAP), and the exponent « Y » is a scale factor. The constants « X » and « Y » are taken from the
404 website (www.matches.com). Exponent values « Y » for other types of equipment can be obtained from
405 other documents such as Chauvel (1981) and Remer and Chai (1990). CEPCI_a is the Chemical Engineering
406 Plant Cost Index (CEPCI) (607.5, Overall average 2019) and CEPCI_o is the original CEPCI value for the year
407 in which equipment costs were evaluated.

408 Once purchase equipment costs were established, the other components of the total investment costs
409 were estimated using multiplying factors called Lang Factors. The direct and indirect costs were combined

1
2
3
4
5
6
7
8
9
10
11
12
13
14
15
16
17
18
19
20
21
22
23
24
25
26
27
28
29
30
31
32
33
34
35
36
37
38
39
40
41
42
43
44
45
46
47
48
49
50
51
52
53
54
55
56
57
58
59
60
61
62
63
64
65

410 to determine the total capital costs. A total investment of 30.67 M CAD\$ was estimated for the present
411 scenario.

412 The direct operating costs include chemical products (www.alibaba.com), labor (25 CAD\$.h⁻¹), electricity
413 (0.07 CAD\$.kWh⁻¹), process water (0.5 CAD\$.m⁻³), maintenance and repairs, operating supplies, and
414 laboratory charges (Table 4). The indirect costs include marginal social benefits, amortization and
415 financing costs. The proportion of various direct and indirect costs relative to the total cost is presented
416 in Figure 6. Total costs are dominated by the financing (interest refund) and amortization costs that
417 represented 39.3% and 23.8% of total cost, while chemicals and labor costs only represented 2.17 and
418 11.4%, respectively. Based on market values reported in 2019, the price for acid grade fluor spar, with a
419 CaF₂ purity greater than 97%, varied from 400 to 500 CAD\$.t⁻¹ (USGS, 2020). In the present study, the
420 purity of the fluor spar by-product obtained after the flotation step was estimated at 95.1%. Therefore,
421 the fluor spar by-product price was fixed at 350 CAD\$.t⁻¹. The total costs (direct and indirect) of the
422 flotation process develop to improve the purity of the fluor spar by-product are estimated at 194 CAD\$.t⁻¹,
423 while the fluor spar by-product revenues obtained are estimated at 244 CAD\$.t⁻¹, indicating that the
424 additional flotation operation is feasible, not only to upgrade fluor spar by-product (from commercial to
425 ceramic grade), but also to generate a profit of at least 50 \$CAD.t⁻¹.

426 **4 Conclusions**

427 The recovery of fluor spar as a by-product of a REE-rich carbonatite deposit could favor the reduction of
428 the volume of potentially problematic metallurgical residues to be disposed, while creating a secondary
429 source of revenue. Depending on its purity, fluor spar by-product can be classified into: i) metallurgical, ii)
430 ceramic or iii) acid grade. In this study, a process consisting of a four steps to separate fluor spar from REE-
431 bearing minerals and other impurities (e.g. silicate minerals) is described. The purity of the fluor spar by-
432 product was increased from very low-grade CaF₂ (15.6% - with no commercial value) to a high-grade CaF₂
433 (95.1% - ceramic grade with an estimated value of 350 CAD\$.t⁻¹). Impurities, such as carbonates were
434 removed by acid (HCl) leaching. Fe- and REE-bearing minerals (magnetic or paramagnetic minerals) were
435 removed from the fluor spar by-product (non-magnetic mineral) during magnetic separation. The flotation
436 step is an important step to remove silicate-bearing minerals (impurities) from the fluor spar by-product
437 and decrease its Si content (<2.5% SiO₂ for ceramic grade and <1.5% SiO₂ for acid grade). A cost-benefit
438 analysis of the flotation step showed that the additional flotation operation is feasible, not only to upgrade

1
2
3
4
5
6
7
8
9
10
11
12
13
14
15
16
17
18
19
20
21
22
23
24
25
26
27
28
29
30
31
32
33
34
35
36
37
38
39
40
41
42
43
44
45
46
47
48
49
50
51
52
53
54
55
56
57
58
59
60
61
62
63
64
65

439 fluorspar by-product (from commercial to ceramic grade), but also to generate a profit of at least
440 50 \$CAD.t⁻¹.

441 **Acknowledgments**

442 This research was supported by the Fonds de Recherche du Québec - Nature et Technologies (FRQNT,
443 Québec's Research Funds – Nature and Technologies), Grant 2017-MI-202293, the Canada Research Chair
444 Program (No. 950-232194), and the industrial partner in the project, Commerce Resources Corp. Sincere
445 thanks to Darren Smith of Commerce Resources Corp. and Yves Thomassin from BBA Consulting Inc. for
446 providing samples, technical support and reviews.

447

References

- Amine, M., Asafar, F., Bilali, L., Nadifiyine, M., 2019. Hydrochloric acid leaching study of rare earth elements from Moroccan phosphate. *Journal of Chemistry* 85, 1-10.
- Bian, X., Yin, S.H., Luo, Y., Wu W.Y., 2011. Leaching kinetics of bastnaesite concentrate in HCl solution. *Transactions of Nonferrous Metals Society of China* 21(10), 2306-2310.
- Chou, L., Garrels, R.M., Wollast, R., 1989. Comparative study of the kinetics and mechanisms of dissolution of carbonate minerals. *Chemical Geology* 78(3), 269-282.
- Corpas-Martínez, J.R., Pérez, A., Navarro-Domínguez, R., Amor-Castillo, C., Martín-Lara, M.A., Calero, M., 2020. Comparison between performance of fluorite flotation under different depressants reagents in two pieces of laboratory equipment. *Applied Sciences* 10, 5667; <https://doi.org.10.3390/app10165667>.
- Coudert, L., Blais, J.F., Mercier, G., Cooper, P., Gastonguay, L., Morris, P., Janin, A., Reynier, N., 2013. Pilot-scale investigation of the robustness and efficiency of a copper-based treated wood wastes recycling process. *Journal of Hazardous Materials* 261, 277-285.
- Council N.R., 2002. *Evolutionary and revolutionary technologies for mining*. The National Academic Press, Washington, DC, USA, 102 p. <https://www.nap.edu/catalog/10318/evolutionary-and-revolutionary-technologies-for-mining>.
- Crundwell, F.K., 2017. On the mechanism of the dissolution of quartz and silica in aqueous solutions. *ACS Omega* 2(3), 1116-1127.
- Eurofluor, 2016. *A snapshot of the fluorine industry*, third ed. European Chemical Industry Council, Brussels, Belgium, 16 p.
- Filippov, L.O., Dehaine, Q., Filippova, I.V., 2016. Rare earths (La, Ce, Nd) and rare metals (Sn, Nb, W) as by-products of kaolin production – Part 3: Processing of fines using gravity and flotation. *Minerals Engineering* 95, 96-106.
- Gagnon, G., 2015. *Preliminary economic assessment Ashram Rare Earth Deposit*. SGS for Commerce Resources Corporation, Vancouver, BC, Canada.
- Habashi, F., 2013. Extractive metallurgy of rare earths. *Canadian Metallurgical Quarterly* 52, 224-233.

1
2
3
4 475 Harben, P.W., 2002. The industrial minerals handbook : A guide to markets, specifications & prices.
5
6 476 Industrial Minerals Information, Worcester Park, Surrey, UK.
7
8 477 Hayes, T.S., Miller, M.M., Orris, G.J., Piatak, N.M., 2017. Fluorine. In: Professional Paper. Schulz, K.J.,
9
10 478 Deyoung, J.J.H., Seal li, R.R., Bradley, D.C. (Editors), U.S. Geological Survey, Reston, VA, USA, 92 p.
11
12 479 Jordens, A., Sheridan, R.S., Rowson, N.A., Waters, K.E., 2014. Processing a rare earth mineral deposit using
13
14 480 gravity and magnetic separation. Minerals Engineering 62, 9-18.
15
16 481 Kampf, A.R., 2003. Handbook of mineralogy, Volume V. Borates, Carbonates, Sulfates. John W. Anthony,
17
18 482 Richard A. Bideaux, Kenneth W. Bladh, and Monte C. Nichols (Editors), Mineral Data Publishing,
19
20 483 Tucson, Arizona, USA, 813 p., American Mineralogist 88(11-12), 1842-1842.
21
22 484 Kursun, I., Terzi, M., Tombal, T.D., 2016. HCl leaching behaviour of a bastnasite ore in terms of thorium
23
24 485 and rare earth elements. Russian Journal of Non-Ferrous Metals 57(3), 187-194.
25
26 486 Liu, H., Khoso, S.A., Sun, W., Zhu, Y., Han, H., Hu, Y., Kang, J., Meng, X., Zhang, Q., 2019. A novel method
27
28 487 for desulfurization and purification of fluorite concentrate using acid leaching and reverse
29
30 488 flotation of sulfide. Journal of Cleaner Production 209, 1006-1015.
31
32 489 Magotra, R., Namga, S., Singh, P., Arora, N., Srivastava, P.K., 2017. A new classification scheme of fluorite
33
34 490 deposits. International Journal of Geosciences 8, 599-610.
35
36 491 Mat Sulji, L., Ibrahim, W., Abdul Aziz, B., Deraman, M.R., Ismail, N., 2017. A review of rare earth mineral
37
38 492 processing technology. Chemical Engineering Research Bulletin 19, 20-35.
39
40 493 Minz, F., Kern, M., Birtel, S., Höfig, T., Krause, J., Gutzmer, J., 2017. Distribution of REE minerals in fluorite
41
42 494 flotation at the Vergenoeg Mine, South Africa. Conference: Process Mineralogy, Cape Town, South
43
44 495 Africa.
45
46 496 Mocellin, J., Mercier, G., Morel, J.L., Charbonnier, P., Blais, J.F., Simonnot, M.O., 2017. Recovery of zinc
47
48 497 and manganese from pyrometallurgy sludge by hydrometallurgical processing. Journal of Cleaner
49
50 498 Production 168, 311-321.
51
52 499 Momota, K., Yamamoto, K., Inoue, Y., Watanabe, S., 2004. Method for producing calcium fluoride, reusing
53
54 500 method and recycling method thereof. Patent pending WO2005070831A1.
55
56 501 Nguyen, T.Y.C., Coudert, L., Tran, L.H., Mueller, K., Mercier, G., Blais, J.F., 2021. Recovery of high-grade
57
58 502 fluorspar by column flotation. J. Cleaner Production (submitted paper).
59
60
61
62
63
64
65

1
2
3
4 503 Nguyen, T.Y.C., Tran, L.H., Mueller, K., Coudert, L., Mercier, G., Blais, J.F., 2021. Pre-concentration of
5
6 504 fluorite from a rare earth element carbonatite deposit through the combination of magnetic
7
8 505 separation and leaching. Minerals Engineering (submitted paper).
9
10 506 Pasquier, L.C., Mercier, G., Blais, J.F., Cecchi, E., Kentish, S., 2016. Technical & economic evaluation of a
11
12 507 mineral carbonation process using southern Québec mining wastes for CO₂ sequestration of raw
13
14 508 flue gas with by-product recovery. International Journal of Greenhouse Gas Control 50, 147-157.
15
16 509 Patnaik, P., 2002. Handbook of inorganic chemicals. McGraw-Hill, New York, NY, USA, 1087 p.
17
18 510 Rosenblum, S., Brownfield, I.K., 2000. Magnetic susceptibilities of minerals. In: Open-File Report 99-529.
19
20 511 U.S. Geological Survey, Reston, VA, USA, 37 p.; <https://doi.org.10.3133/ofr99529>.
21
22 512 Solihin, Indriani, Mubarok, Z., 2018. Dissolution profile of dolomite in chloric acid solution: The effect of
23
24 513 chloric acid concentration and pulp density. Conference: Proceedings of the International Seminar
25
26 514 on Metallurgy and Materials (ISMM2017): Metallurgy and Advanced Material Technology for
27
28 515 Sustainable Development. May 2018AIP Conference Proceedings 1964(1):020022;
29
30 516 DOI.10.1063/1.5038304.
31
32 517 USGS, 2020. Fluorspar – Mineral Commodity summaries 2019.
33
34 518 <https://www.usgs.gov/centers/nmic/fluorspar-statistics-and-information> (Consulted April, 10,
35
36 519 2020).
37
38 520 Wenliang, X., Bingyan, C., 2011. Flotation recovery of fluorite from rare earth operation taillings. 2011
39
40 521 International Conference on Remote Sensing, Environment and Transportation Engineering. June,
41
42 522 24-26, 2011, pp. 3163-3166.
43
44 523 Woolley, A., Kjarsgaard, B., 2008. Carbonatite occurrences of the world: Map and database. Geological
45
46 524 Survey of Canada. Open File 5796; <https://doi.org/10.4095/225115>.
47
48 525 Xiong, W., Deng, J., Chen, B., Deng, S., Wei, D., 2018. Flotation-magnetic separation for the beneficiation
49
50 526 of rare earth ores. Minerals Engineering 119, 49-56.
51
52 527 Ye, J., Yang, D.C., 1992. Packed column flotation for fluorspar beneficiation. Mining, Metallurgy &
53
54 528 Exploration 9(4), 196-199.
55
56 529
57
58 530
59
60
61
62
63
64
65

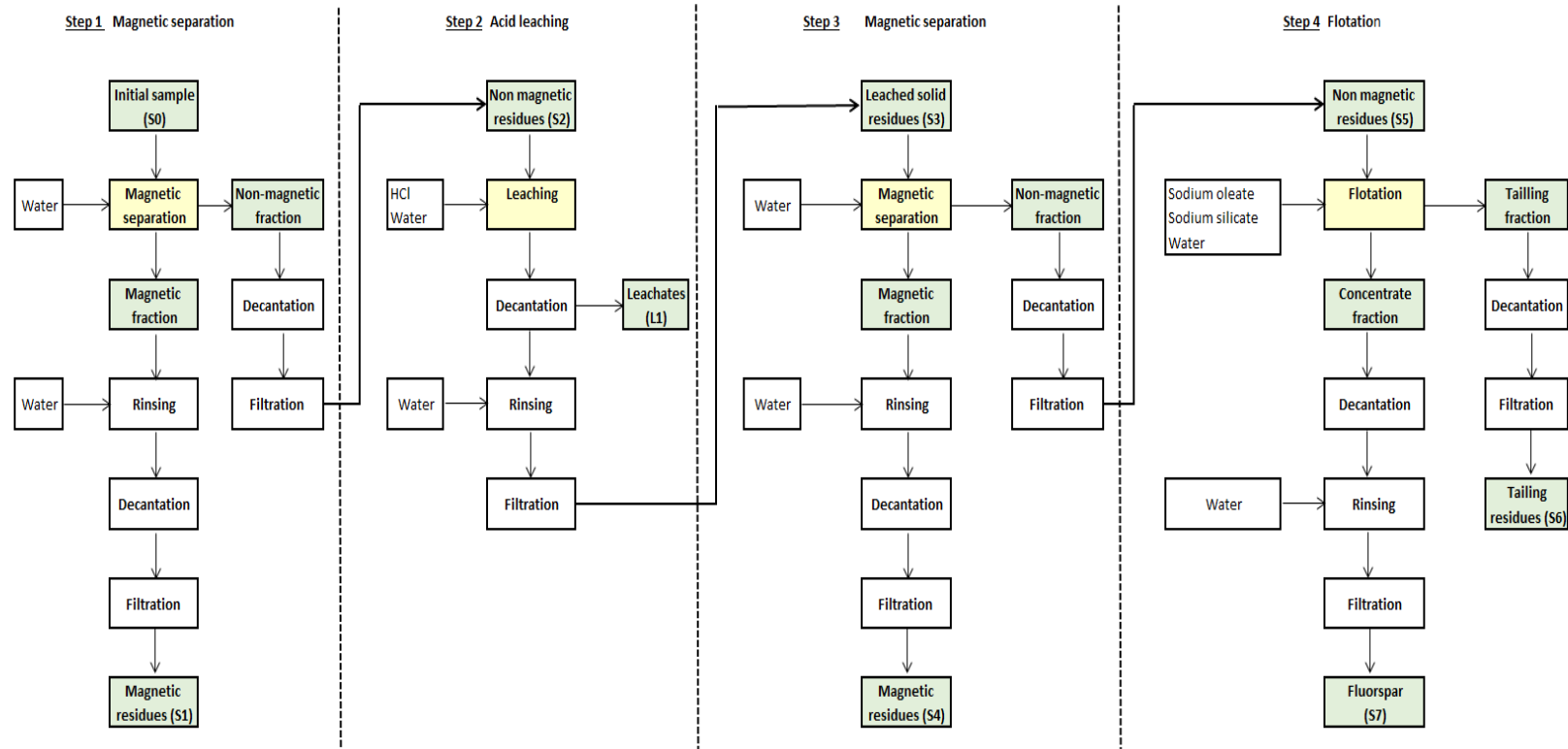
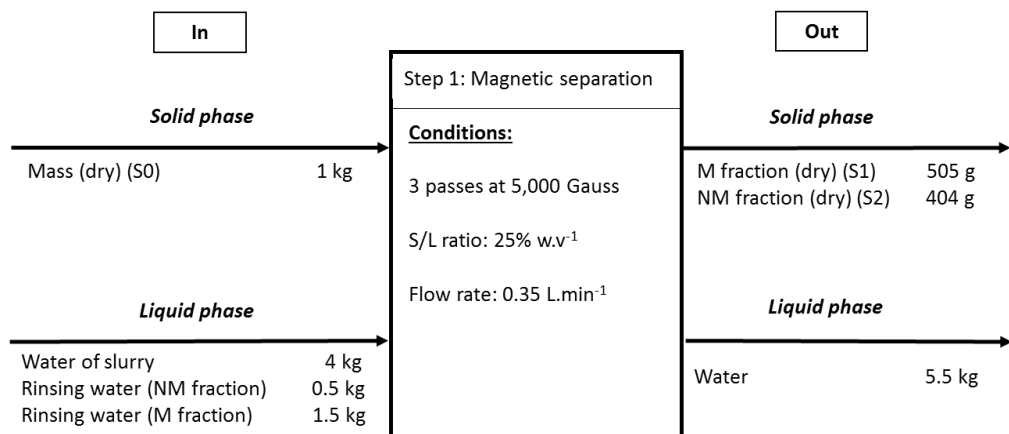
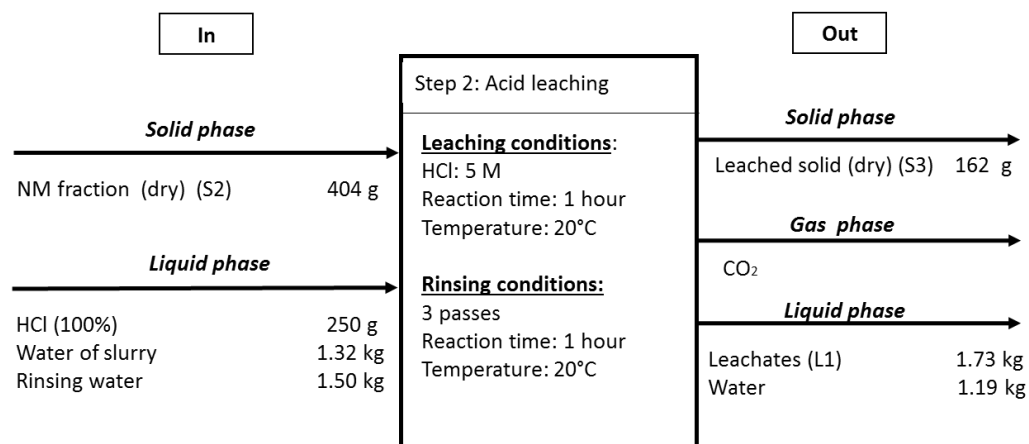


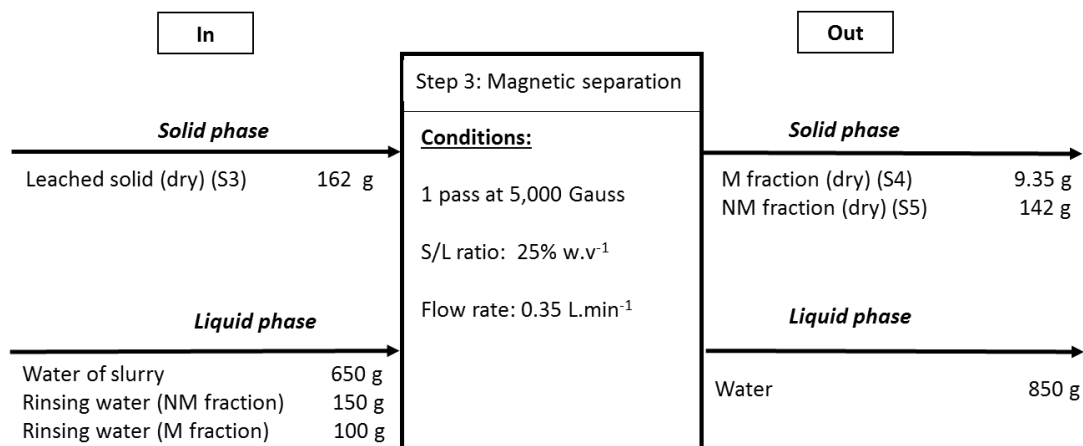
Figure 1 Detailed flowsheet of the proposed complete fluor spar purification process



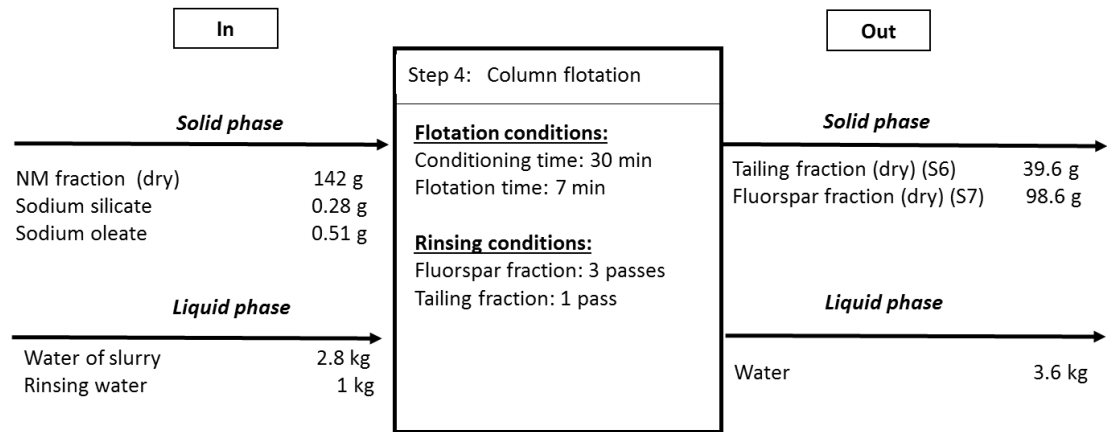
a.



b.



c.



d.

Figure 2 Input and output of each unit operation of fluorspar process: a.- step 1 magnetic separation; b.- step 2 acid leaching; c.- step 3 magnetic separation; d.- step 4 column flotation

(NM fraction: non-magnetic fraction; M fraction: magnetic fraction)

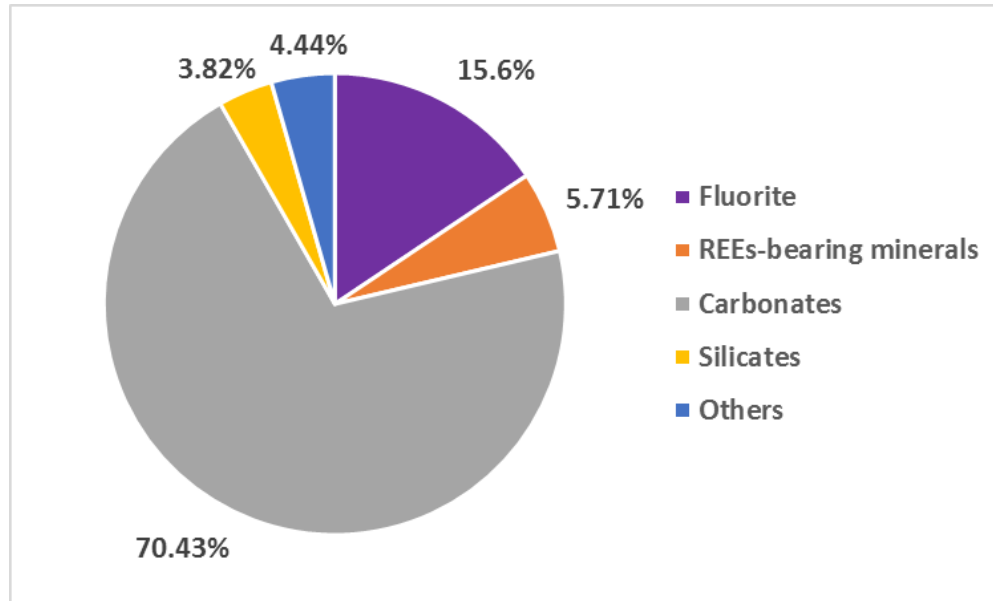


Figure 3 Mineralogical composition of the initial sample (S0)

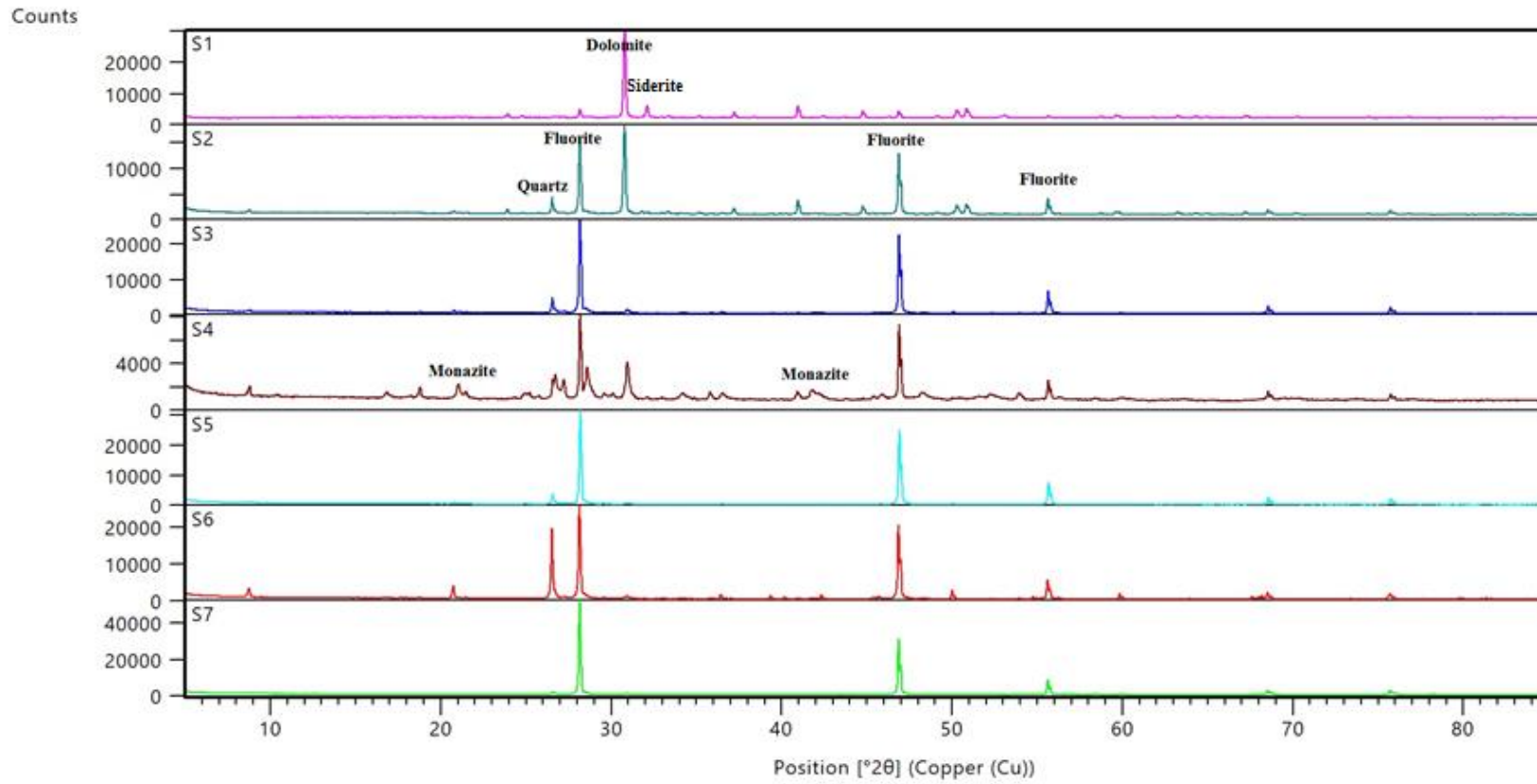


Figure 4 XRD patterns of the solid samples after each step of the fluorspar purification process

S1-magnetic fraction (step 1); S2-non-magnetic fraction (step 1); S3-leached solid sample (step 2); S4: magnetic fraction (step 3); S5-non-magnetic fraction (step 3); S6-tailing fraction (step 4); S7- concentrate fraction (step 4)

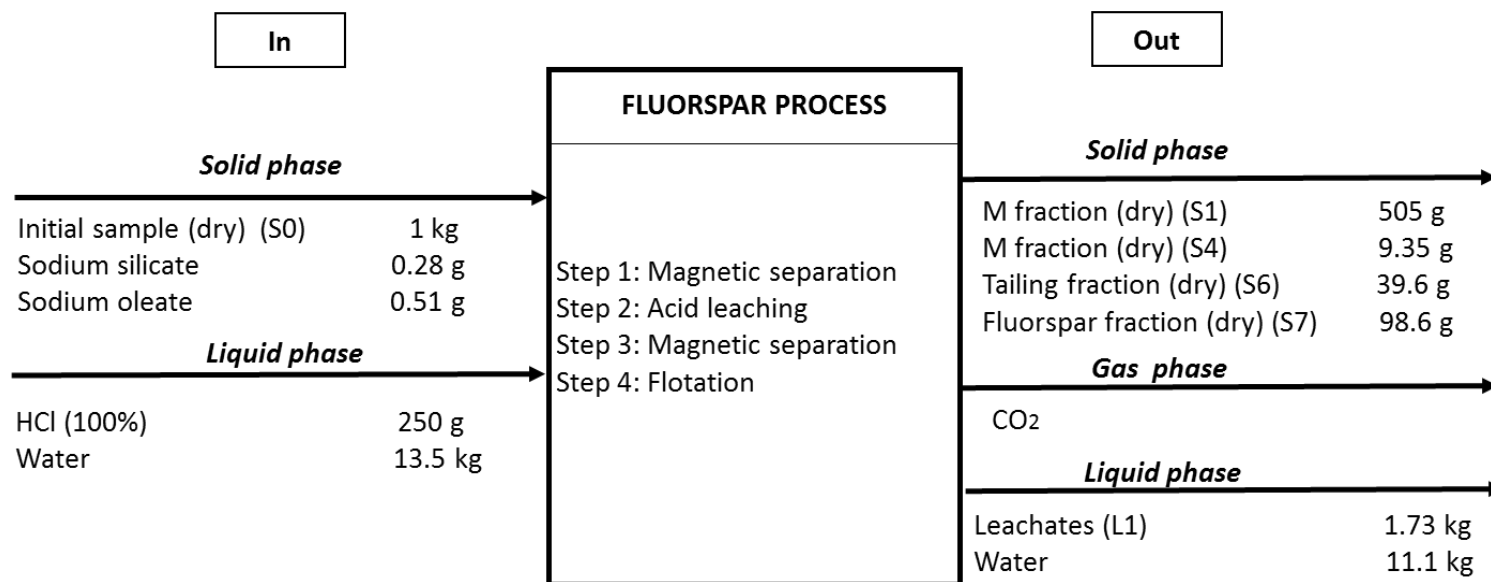


Figure 5 Mass balance per kg of solid treated by fluorspar purification process

(M fraction: magnetic fraction; NM: non-magnetic fraction)

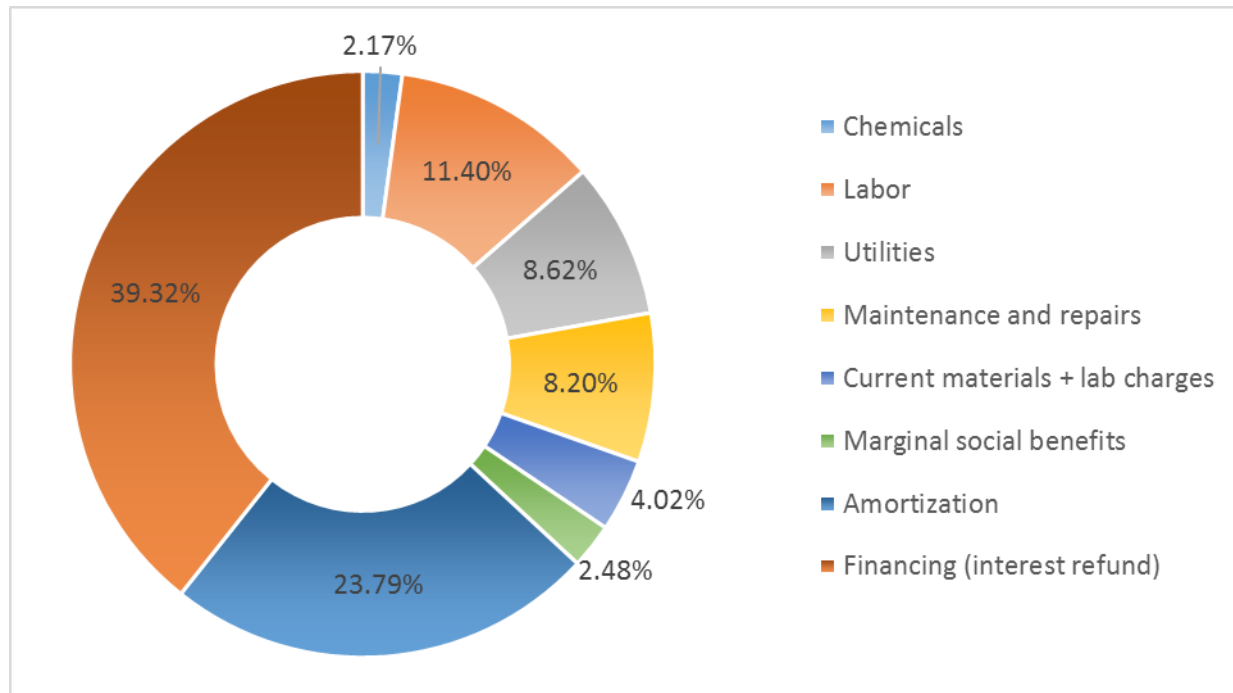


Figure 6 Total cost analysis for the production of a fluorspar by-product from a REE-bearing carbonate deposit using flotation

Table 1 Element content (%) in solid sample before (S0) and after each unit operation (S1 to S7) of the fluorspar purification process

Elements (%)	Ca	F	Mg	Fe	Si	REEs	C
S0	21.8 ± 1.2	9.14 ± 0.59	5.94 ± 0.07	6.98 ± 0.24	1.44 ± 0.13	2.45 ± 0.34	7.13 ± 0.68
S1	22.2 ± 4.2	4.71 ± 1.01	6.51 ± 1.89	8.28 ± 1.59	0.54 ± 0.24	2.77 ± 0.23	8.26 ± 0.63
S2	25.2 ± 4.9	17.5 ± 0.9	4.84 ± 0.63	4.26 ± 0.37	2.46 ± 0.38	2.21 ± 0.71	7.14 ± 0.53
S3	35.8 ± 1.5	37.0 ± 2.4	0.35 ± 0.02	0.40 ± 0.03	5.07 ± 0.15	3.91 ± 1.31	0.19 ± 0.18
S4	26.1 ± 2.9	25.4 ± 2.7	0.98 ± 0.13	1.62 ± 0.35	2.98 ± 0.63	25.9 ± 1.6	-
S5	38.7 ± 0.6	39.3 ± 1.7	0.29 ± 0.07	0.32 ± 0.05	5.55 ± 0.21	2.44 ± 0.95	-
S6	33.4 ± 2.7	26.9 ± 0.9	0.39 ± 0.04	0.40 ± 0.06	14.9 ± 0.1	2.94 ± 0.62	-
S7	45.7 ± 1.2	45.1 ± 1.7	0.10 ± 0.01	0.27 ± 0.06	1.15 ± 0.11	1.81 ± 0.62	-

Table 2 Mass balance, overall recovery and grade of fluorspar and REEs from fluorspar purification process

		Mass (g)	Fluorspar		Rare earth elements	
			Grade (%) *	Mass recovery (%)	Grade (%) **	Mass Recovery (%)
Input	S0	1000	18.8 ± 1.2	100	2.45 ± 0.34	100
Output	S1	505 ± 8	9.68 ± 1.87	26.3	2.77 ± 0.23	57.1
	L1	176 ± 3	0.86 ± 0.65	0.8	0.42 ± 0.13	3.1
	S4	9.4 ± 1.0	52.2 ± 5.6	3.95	25.9 ± 1.6	9.9
	S6	39.6 ± 1.2	55.5 ± 1.9	13.4	2.94 ± 0.62	4.8
	S7	98.6 ± 1.7	92.8 ± 3.6	50.3	1.81 ± 0.62	7.0
Output/Input (%)				94.0		82.0

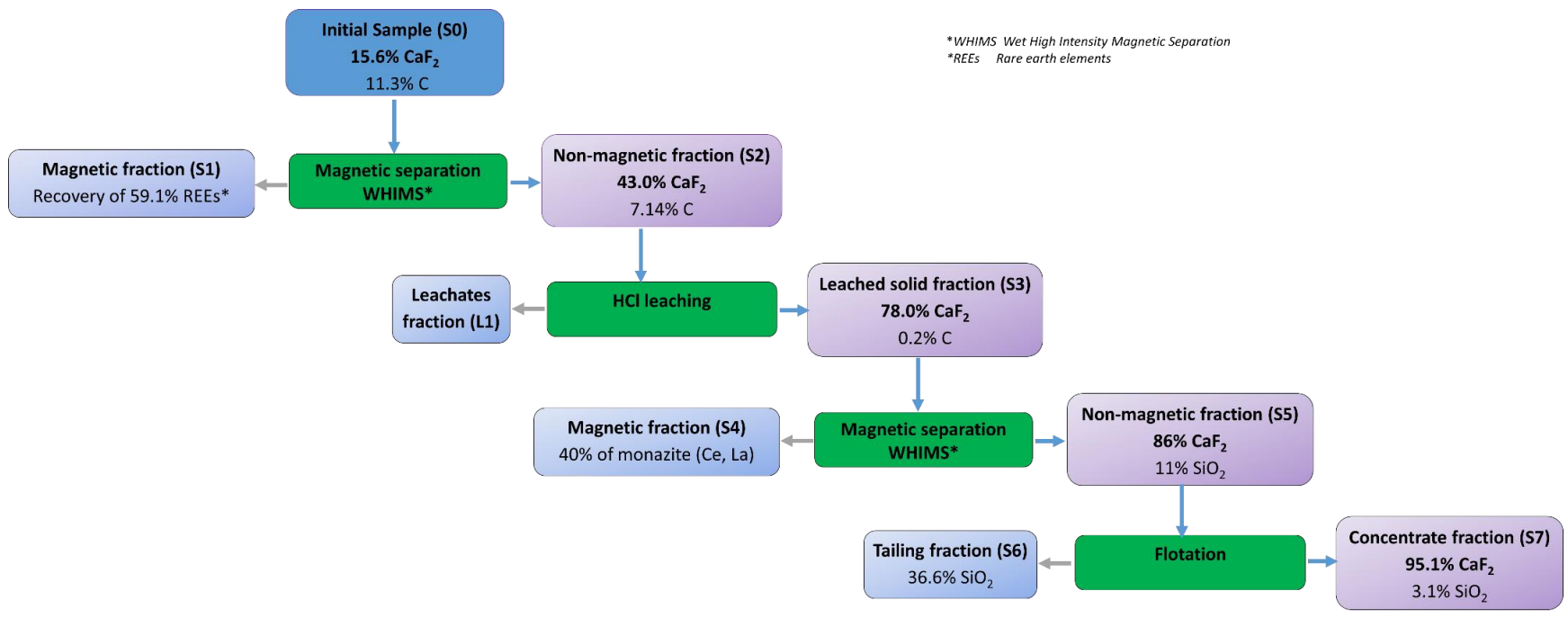
*Fluorspar grade estimated by fluorine content; **REEs estimated by the sum of Ce, La, Y content.

Table 3 Basic operating, market, and capitalization parameters of the techno-economic model for the flotation process developed to purify a fluorspar by-product from a REE-bearing carbonatite deposit

Parameters	Values	Units
Basic operating parameters		
Operating period	350	d.yr ⁻¹
Processing capacity of a plant	100	t.d ⁻¹
Daily operation period	24	h.d ⁻¹
Factor of safety (for equipment)	20	%
Market parameters		
Annual inflation rate	2.0	%.yr ⁻¹
Annual interest rate	4.5	%.yr ⁻¹
Annual discount rate	6.0	%.yr ⁻¹
Income tax	30	% of gross income
Exchange rate	1.25	\$US / \$CAD
Chemical Engineering Plant Cost Index	607.5	Average 2019
Capitalization parameters		
Amortization period	20	yr
Lifetime of equipment	20	yr
Direct costs		
Equipment		
<i>Insulation installation equipment</i>	19	%
<i>Instrumentation and control</i>	3	%
<i>Piping and pipeline systems</i>	7	%
<i>Electrical system</i>	8	%
Building process and services	10	%
Landscaping	2	%
Facilities and services	10	%
Indirect costs		
Engineering and supervision	32	%
Construction spending	10	%
Construction management fees	9	% cap. (dir. + indir.)
Contingent fees	26	% cap. (dir. + indir.)
Working capital	15	% fixed capital costs

Table 4 Economic evaluation of the flotation process developed to purify a fluorspar by-product from REE-bearing carbonatite deposit

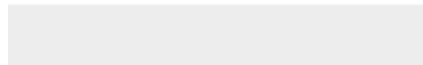
Parameters	Values	Units	Cost (-)/profit (+) (CAD\$.t ⁻¹)
Direct operating costs			-66.6
Chemicals			
Sodium silicate	0.30	CAD\$.kg ⁻¹	-0.6
Sodium oleate	1.00	CAD\$.kg ⁻¹	-3.6
Labor			
Technicians	25.0	CAD\$.h ⁻¹	-18.4
Supervision	20.0	% (labor cost)	-3.7
Utilities			
Electricity	0.07	CAD\$.kWh ⁻¹	-16.5
Water process	0.50	CAD\$.m ⁻³	-0.2
Maintenance and repairs	2.00	% fixed cap. costs yr ⁻¹	-15.9
Current materials	0.75	% fixed cap. costs yr ⁻¹	-6.0
Laboratory charges	10	% operating labor	-1.8
Indirect and General costs			-127.2
Marginal social benefits	22.0	% oper. labor + superv.	-4.8
Amortization			-46.1
Financing (interest reimbursement)			-76.2
Mineral revenues			+244.4
Fluorspar by-product	0.35	CAD\$.kg ⁻¹	+244.4
Profit			+50.4





[Click here to access/download](#)

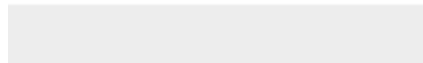
Supplementary files (e-component)
Supplementary Figure 1.docx





[Click here to access/download](#)

Supplementary files (e-component)
Supplementary Figure 2.docx



Declaration of interests

The authors declare that they have no known competing financial interests or personal relationships that could have appeared to influence the work reported in this paper.

The authors declare the following financial interests/personal relationships which may be considered as potential competing interests:

Credit author statement

Authors :

- Thi Yen Chau Nguyen (Conceptualization, Methodology, Investigation, Formal analysis, Roles/Writing - original draft)
- Lan-Huong Tran (Methodology, Writing - review & editing)
- Lucie Coudert (Supervision, Writing - review & editing)
- Kristin Mueller (Writing - review & editing)
- Guy Mercier (Supervision, Writing - review & editing)
- Jean-François Blais (Funding acquisition, Project administration, Supervision, Writing - review & editing)